

What is the origin of slow relaxation modes in highly viscous ionic liquids?

Eliassen, Kira L.; Gabriel, Jan; Blochowicz, Thomas; Gainaru, Catalin P.; Christensen, Tage E.; Niss, Kristine

Published in:
Journal of Chemical Physics

DOI:
[10.1063/5.0215661](https://doi.org/10.1063/5.0215661)

Publication date:
2024

Document Version
Peer reviewed version

Citation for published version (APA):
Eliassen, K. L., Gabriel, J., Blochowicz, T., Gainaru, C. P., Christensen, T. E., & Niss, K. (2024). What is the origin of slow relaxation modes in highly viscous ionic liquids? *Journal of Chemical Physics*, 161(3), Article 034506. <https://doi.org/10.1063/5.0215661>

General rights

Copyright and moral rights for the publications made accessible in the public portal are retained by the authors and/or other copyright owners and it is a condition of accessing publications that users recognise and abide by the legal requirements associated with these rights.

- Users may download and print one copy of any publication from the public portal for the purpose of private study or research.
- You may not further distribute the material or use it for any profit-making activity or commercial gain.
- You may freely distribute the URL identifying the publication in the public portal.

Take down policy

If you believe that this document breaches copyright please contact rucforsk@kb.dk providing details, and we will remove access to the work immediately and investigate your claim.

What is the Origin of Slow Relaxation Modes in Highly Viscous Ionic Liquids?

Kira L. Eliassen¹, Jan Gabriel¹, Thomas Blochowicz², Catalin P. Gainaru³, Tage E. Christensen¹, and Kristine Niss^{1*}

¹ *"Glass and Time", IMFUFA, Department of Science and Environment, Roskilde University, Roskilde, 4000, Denmark*

² *Institut für Festkörperphysik, Technische Universität Darmstadt, Darmstadt, 64289, Germany and*

**Corresponding author, kniss@ruc.dk*

(Dated: June 26, 2024)

"This article may be downloaded for personal use only. Any other use requires prior permission of the author and AIP Publishing. This article appeared in Kira L. Eliassen, Jan Gabriel, Thomas Blochowicz, Catalin P. Gainaru, Tage E. Christensen, Kristine Niss; What is the origin of slow relaxation modes in highly viscous ionic liquids?. J. Chem. Phys. 14 July 2024; 161 (3): 034506 and may be found at <https://doi.org/10.1063/5.0215661>

Abstract

Room temperature ionic liquids (RTILs) are molten salts consisting entirely of ions, and have over the past decades gained increased interest due to their high potential in applications. These structurally complex systems often display multiple relaxation modes in the response functions at lower frequencies, hinting to complex underlying mechanisms.

While the existence of these multimodal spectra in the shear mechanical, dielectric and light scattering response of RTILs has been confirmed multiple times, controversy still surrounds the origin. This paper therefore aims to provide additional insights on the multimodal spectra seen in RTILs by presenting new shear mechanical results on seven different RTILs; Pyr1*n*-TFSI with $n = 4, 6$ and 8 , Pyr18-TFSI mixed with Li-TFSI in two high concentrations, and C_{*n*}-mim-BF₄ with $n = 3$ and 8 . Dynamic depolarized light scattering was also measured on one of the Pyr18-TFSI Li-salt mixtures. These specific cases were analyzed in detail and put into a bigger perspective together with an overview of the literature.

Recent literature offers two specific explanations for the origin of the multimodal shear mechanical spectra; 1) cation-anion time scale separation or 2) combined cation-anion relaxation in addition to a dynamic signal from mesoscale aggregates at lower frequencies. However, neither of these two pictures can consistently explain all the results on different ionic liquids. Instead we conclude that origin of the multimodal spectrum is system specific. This underlines the complexity of this class of liquids and shows that great care must be taken when making general conclusions based on specific cases.

Keywords: Glass transition, viscous liquids, ionic liquids, slow relaxation, slow mode, mesoscale aggregates, dynamic mechanical spectroscopy, shear modulus, dielectric spectroscopy, depolarized dynamic light scattering

I. INTRODUCTION

Room temperature ionic liquids (RTILs) are salts that are molten at room temperature and therefore consist entirely of ions. They form a diverse and interesting class of liquids, which has attracted considerable attention over the last decades due to their unique properties such as a broad electrochemical window and liquid temperature range, negligible vapor pressure and non-flammability [1, 2]. They often consist of an organic cation of low symmetry and an inorganic anion. The particularities of the ionic structure and the combinations of different cations and anions leads to a huge variety of this class

of liquids, and a large range of desired properties can therefore be obtained [3].

This wide range of properties makes ionic liquids candidates for many technological areas, e.g. in energy applications such as rechargeable batteries, solar cells, fuel cells and supercapacitors [4–9], synthesis [4, 7], processing of biomolecules like cellulose [10, 11] and several other applications [12]. To fully exploit the application potential, a better understanding of the connection between chemical structure and properties of the ionic liquids is needed. As for other liquids the properties are tightly coupled to the dynamics. Close to room temperature the dynamics take place on the picosecond to microsecond time scale. This fast dynamics is typically studied with NMR [13–15] and neutron scattering [16–19] as well as with MD simulations [13–15, 20–22].

While the room temperature properties are the most interesting from a direct application perspective it is also interesting to understand the dynamics of ionic liquids at lower temperatures where the dynamics is much slower. Many ionic liquids can readily be super-cooled and brought all the way into the glassy state [23–26]. Glasses are formed because the main relaxation, the alpha relaxation slows down upon cooling and the viscosity grows. The glass transition temperature, T_g , is defined as the temperature where the alpha relaxation time reaches a 1000 seconds and the viscosity is 10^{12} Pas. In the temperature range above the glass transition the dynamics is slow compared to non-viscous liquids and ranges from the millisecond to kilosecond range [23–26]. Slow dynamics and glass formation are observed across a wide array of chemically diverse systems, ranging from metals to polymers. However, the mechanisms governing these slow dynamical processes remain unclear [27–30] A key question is what the role of specific chemical compositions and microscopic structures is in these processes. Ionic liquids present a particularly interesting class of glass-forming liquids, as their behavior is influenced by both Coulombic and van der Waals interactions.

In shear rheology, on the low-frequency side of the alpha relaxation peak, the spectrum of simple (non-polymeric, non-associated) liquids display the so-called terminal Maxwell mode, which marks the transition to fully viscous behavior. In some ionic liquids, however, it has been shown that there are additional slow relaxation contributions intermediate between the alpha relaxation and the terminal mode [31–34], giving rise to multimodal spectra. Multimodal spectra are also observed with other experimental techniques such as dielectric spectroscopy [26, 32, 35] and dynamic light scattering [26]. Furthermore, some RTILs have additional short time (high frequency) modes in the dielectric [36] and shear

mechanical responses [23] as also seen in other classes of glassforming liquids [37–39].

This paper focuses on relaxation modes slower than the alpha relaxation. Other types of glass-forming liquids also exhibit modes slower than the alpha relaxation. Over the last few decades, it has been established that a slow mode is observed in mono-hydroxy alcohols and sometimes in polyalcohols and amines [38, 40–42]. In the case of mono-hydroxy alcohols, it is most clearly observed as a prominent slow mode in the dielectric signal, referred to as Debye relaxation, characterized by an (almost) perfect exponential relaxation spectrum [40]. The slow mode in alcohols is believed to be due to the dynamics of the hydrogen-bonding network and is interpreted as a polymer-like slow mode [40]. Recent research has identified additional slow modes in polymers and molecular liquids, known as the slow Arrhenius process (SAP), which do not appear to be connected to any long-range structures [43, 44].

To unravel the underlying mechanism governing the spectral complexity of ionic liquids, it is important to note that they offer unique insight into the coupling between structure and dynamics in liquids [45]. In relation to this, it should be noted that ionic liquids are, by definition, binary liquids, but unlike other binary liquids/mixtures there is no possibility of phase separation, not even on a nanoscale level, due to the requirement of local charge neutrality. As opposed to simple molecular liquids where there is usually only one peak in the x-ray structure factor, in RTILs the latter display three distinct peaks. The two peaks at higher q -values are present in almost all ionic liquids, but the third peak at low q -values is only present in some cases. The peak at highest q -values is the main peak/adjacency peak related to the nearest neighbor correlation. This is the one also present in conventional solvents such as methanol [46]. The intermediate peak is the charge alternation peak, arising from the alternation of charges in the cation and anion. This peak is the signature of an ionic compound such as a RTIL, where Coulomb interactions play an important role. However, there are certain cases where it is not visible in x-ray structure factor due to anti-correlation effects leading to a phase cancellation in the structure factor [46]. The peak at lowest q -values is related to polarity alternation and is often referred to as the pre-peak [47].

The polar regions consist of the head of the cation plus the anion, while the apolar regions consist of the alkyl chains of the cation. It is understood, that when the alkyl chain is butyl, or longer, a sponge-like structure forms where the polar parts of the molecules connect in a network, with a clear separation to islands of apolar regions, and

these structures are often referred to as mesoscale aggregates. This is the alternation that with some periodicity is giving rise to the pre-peak [48] in the structure factor. This pre-peak was first experimentally discovered in 2007 [49] and since confirmed in several experimental and simulation studies [48, 50–54]. The pre-peak associated with the polar-apolar regions is generally present in ionic liquids where the cation has an alkyl chain of four carbons or more [55]. Below the critical length of four carbon atoms in the alkyl chain, the liquid structure is understood to be more homogeneous with no distinct polar-apolar alternations [52, 55].

The focus of this paper is the dynamics of RTILs and in particular the different relaxation modes that are observed at longer time-scales, i.e. around the structural relaxation and slower than this, and how to assign these relaxation modes to structures at different length scales.

An obvious approach would be to identify if a slower relaxation mode, that are sometimes observed in RTILs, is related to the mesoscale aggregates found in some RTILs. This slower relaxation mode is often referred to as the slow mode, and if the origin is different from the main, structural relaxation of the ionic liquid, it could be due to dynamics from the mesoscale aggregates. This would be analogous to the case for the slow mode found in some alcohols, where the slow mode as mentioned above is considered to be the dynamics of supramolecular hydrogen-bonding structures [40–42].

One could on the other hand also consider other explanations for the multimodal relaxation spectra observed with different experimental techniques. As mentioned above, RTILs are structurally complex, binary liquids with structures on several length scales and identifying the dynamic signature of these is no simple matter. Added to this complexity is also the fact that the different experimental techniques are sensitive to different aspects of the dynamics.

In order to move forward, the rest of this introduction will therefore give an overview of the current knowledge about the slower relaxation modes in RTILs, and how these are interpreted. This overview is also necessary since even though several slower relaxation modes in the spectrum of various RTILs has been observed with broadband dielectric spectroscopy (BDS), dynamic mechanical spectroscopy (DMS) and depolarized dynamic light scattering (DDLs) in several studies going back to 2011, there is to this day not consensus in the interpretation of these slow relaxations.

One interpretation in literature is that the slowest dynamic mode is the dynamic signal

of long-lived mesoscale aggregates. Several studies support this interpretation simply due to the fact that the time scale of the slow mode is slower than the alpha/main relaxation [31, 32, 56]. Another, more detailed, argument for this interpretation is that the onset of a slow mode in a homologous series of RTILs, i.e. a series with increasing alkyl chain length, matches the onset of the pre-peak in the x-ray structure factor. This match could indicate a similar origin, which would be the mesoscale aggregates, since the pre-peak has been found to be directly linked to these [51].

More complex arguments for this interpretation are also presented in literature. One is that the time scale of the slower mode matches that of mesoscale aggregates as directly probed by neutron-spin echo measurements [32]. Another is that there is a systematic change in the dielectric strength parameter with a systematic change in alkyl chain length, and this can be directly linked to changes in the shape of the mesoscale aggregates [33, 34].

Fewer studies come with another interpretation of the multimodal spectra sometimes seen in RTILs. One alternative interpretation of the bimodal spectra seen in the shear mechanical response of Omim-BF₄ is that the appearance of a slower mode in addition to the main relaxation mode is simply due to a separation of cation and anion relaxation times, resulting in a bimodal spectrum with not one but two alpha relaxations [26]. This argument was supported by comparing the relaxation spectrum across different response functions. In fact, this study observe a third relaxation mode at even lower frequencies, and connects this mode to the mesoscale aggregates.

Another study tested the pressure dependence of bimodal spectrum mode seen in the dielectric permittivity of two different RTILs and compared it to the pressure dependence of the pre-peak. They observed that the slower mode did not follow the same trend as the pre-peak upon compression [35]. Consequently, the origin of the pre-peak and the slower mode has to be different. In fact, the authors found that the origin of the bimodal spectrum was most likely a separation of the rotational and translational dynamics.

The above overview of literature shows that more targeted research is required to reveal the nature of the multimodal spectrum sometimes observed in RTILs. This study will in detail go through new results to further investigate the connection between low-frequency modes in the shear mechanical response and the mesoscale aggregates.

This was done by comparing the behavior of the slower mode in a bimodal spectrum with that of the structure factor pre-peak in three different series of RTILs; 1) Pyr1*n*-TFSI with $n = 4, 6$ and 8 , 2) Pyr18-TFSI mixed with Li-salt and 3) C_{*n*}mim-BF₄ with

$n = 3$ and 8. The x-ray structure factor for these three series of ionic liquids can be seen in figure 1. All three plots of the structure factor show the same tendency; that the pre-peak increases and the charge peak decreases significantly with both increasing alkyl chain length and increased Li-salt concentration.

In this study it was found that there is no obvious connection between the change in the pre-peak with changing alkyl chain length/Li-salt concentration and the appearance/intensity of the slower mode in the shear mechanical spectra. This indicates that the origin of the slower mode is somewhat more complicated and system specific, at variance with what has previously been suggested in literature. Furthermore, the specific cases in this paper will be analysed both in detail and in a larger perspective, giving a solid overview of the nature of the low-frequency modes in ionic liquids.

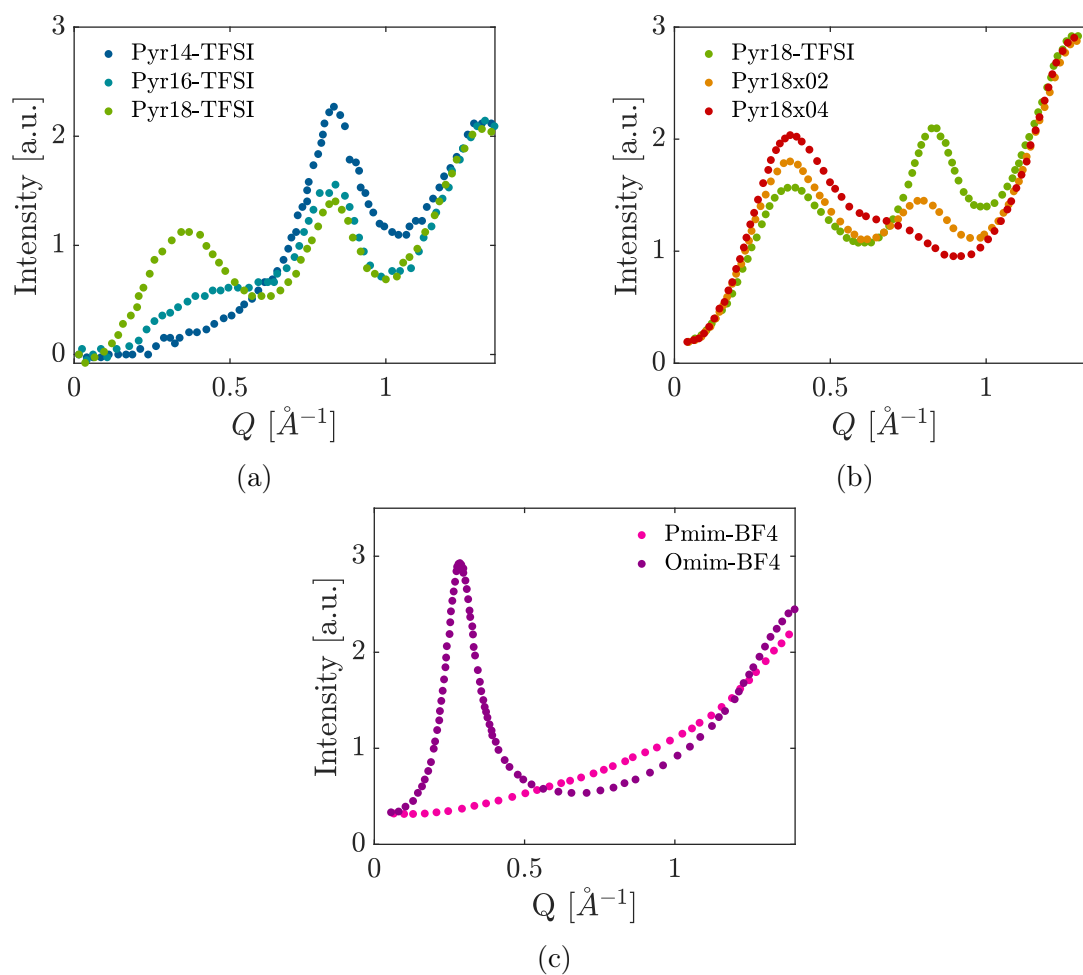


Figure 1: X-ray scattering structure factor for the three series of RTILs to show the development of the scattering pre-peak. a) Pyr1 n -TFSI, b) Pyr18-TFSI mixed with Li-salt, i.e., $(1 - x)$ Pyr18- x Li-TFSI with $x = 0.2$ and 0.4 , and c) is C_n mim-BF $_4$ with $n = 3$ and 8. Data from a), b), and c) are from [51], [53], and [54], respectively. When comparing the two different measurements of neat Pyr18-TFSI (green), they were shown to have the similar peak positions.

II. EXPERIMENTAL DETAILS

A. The samples

The liquids measured in this work were: 1) 1-alkyl-1-methylpyrrolidinium bis(trifluoromethanesulfonyl)imide, $\text{Pyr}1n\text{-TFSI}$, with $n = 4, 6$ and 8 . 2) $\text{Pyr}18\text{-TFSI}$ mixed with Lithium-TFSI, i.e. $(1 - x)\text{Pyr}18\text{-}x\text{Li-TFSI}$, in molar fractions of $x = 0.2$ (denoted $\text{Pyr}18x02$) and $x = 0.4$ (denoted $\text{Pyr}18x04$). 3) 1-alkyl-3-methylimidazolium tetrafluoroborate, $\text{C}_n\text{mim-BF}_4$, with $n = 3$ (Pmim-BF_4) and 8 (Omim-BF_4). $\text{Pyr}1n\text{-TFSI}$ and Li-TFSI were of 99.9% purity and purchased from Solvionic. Omim-BF_4 and Pmim-BF_4 was of 99.8% and above 98% purity, respectively, and both purchased from IoLiTec. All ionic liquids were used as received and stored and prepared in a glove box of dry, inert nitrogen atmosphere to avoid contamination by absorbing moisture from the air, since ionic liquids are known to be very hygroscopic [47]. For an overview of the chemical structures of the measured ionic liquids, see figure 2.

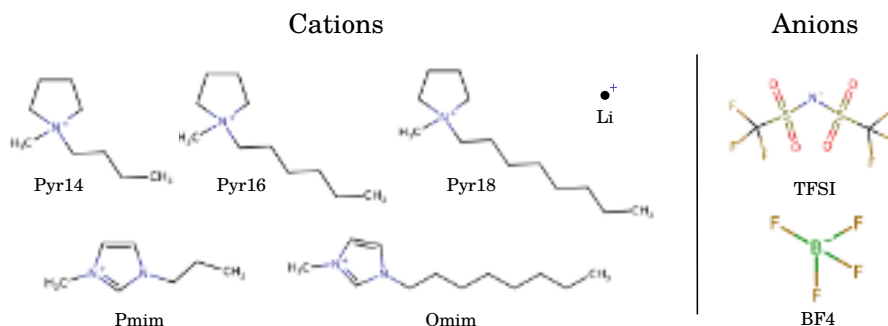


Figure 2: Chemical structures of the molecules forming the ionic liquids measured in this work.

These liquids have been studied to some extent before in literature, with various experimental techniques [18, 19, 24, 32, 49, 53, 54, 57–66] and simulations [46, 67]. Prior to measurements performed with dynamic mechanical and broadband dielectric spectroscopy, all ionic liquids were characterized with thermalization calorimetry (TC) [68] to obtain the glass transition temperature, T_g , and the melting temperature, T_m . The latter arose due to some of the ionic liquids tendency to cold-crystallize during heating, while others were less prone to crystallize and thus gave no measurable T_m .

The TC method works by quench cooling the sample and then measure the heat flow while passively heating to room temperature, giving a ramping rate of around 10 K/min in the temperature range around T_g . The resulting characteristic temperatures can be

seen in table I.

Liquid	T_g [K]	T_m [K]
Pyr14-TFSI	184	254
Pyr16-TFSI	186	285
Pyr18-TFSI	191	259
Pyr18x02	203	273
Pyr18x04	220	nan
Pmim-BF4	180	nan
Omim-BF4	189	nan

Table I: The two characteristic temperatures in the seven measured RTILs; glass transition, T_g , and melting temperature, T_m , as measured with thermalization calorimetry [68]. T_g is observed to systematically increase with both increasing alkyl chain length and Li-salt concentration.

To compare the results from the RTILs with those displayed by a "simple" liquid, the non-associated molecular liquid tetramethyltetra-phenyltrisiloxane (DC704) was measured as well with the same experimental techniques. DC704 has very simple dynamic behavior and exhibit almost complete time-temperature superposition (TTS) with no dynamic modes slower than the alpha relaxation [28, 69–71].

B. Dynamic mechanical spectroscopy

All seven RTILs, as well as DC704, were measured with dynamic mechanical spectroscopy (DMS), giving the frequency dependent shear modulus response; $G^* = G' + iG''$. Broadband DMS measurements were performed at Department of Science and Environment, Roskilde University, Denmark, with the in-house developed rheometer, the Piezo-electric Shear modulus Gauge (PSG) [72]. A special version of the PSG optimized for the use of conducting materials was used in this study [73].

The PSG can measure the shear mechanical response in a shear modulus range of 1MPa to 10 GPa and frequency range of more than seven decades (1mHz to 50 kHz). This gives a unique broadband DMS response unmatched by conventional rheometers, which can measure up to around 100 Hz. In this study, however, the focus is on the low frequency end of the spectrum in order to investigate the slow mode, as was also done

previously using PSG data in a study of supramolecular structures in hydrogen-bonding liquids [38, 42].

The capacitance of the PSG device was measured in a closed-cycle cryostat [74] using the setup as described in Ref. [75]. The cryostat was prior to all measurements purged and filled with dry nitrogen and subsequently sealed, in order to minimize water absorption during measurements.

Pyr14-TFSI, Pyr16-TFSI, Pyr18-TFSI, and Pyr18x02 have a high tendency to cold-crystallize and were consequently cooled rapidly down below the temperature region where the liquids were prone to cold-crystallization and measured in cooling down to around T_g . Pyr18x04, Omim-BF₄ and Pmim-BF₄ did not cold-crystallize in this work, but were still measured upon cooling from the temperature where the alpha relaxation enters the experimental window and down to T_g . Shear mechanical spectra were in all cases measured in the super-cooled state of the ionic liquids in steps of 2 K, with two frequency sweeps at each temperature with a waiting time of 10 minutes in between, to ensure that no crystallization was taking place during the measurements.

To extend the resolution range of PSG results toward low shear modulus values, low frequency oscillatory shear mechanical measurements were performed on Pyr14-TFSI and Pyr18-TFSI at the Technical University of Dortmund using a conventional Anton Paar MCR 502 rheometer with parallel plate geometry having a diameter of 4 and 8 mm. With this setup, the sample was kept dry by a constant flow of nitrogen.

C. Broadband dielectric spectroscopy

The frequency dependent, complex dielectric permittivity, $\varepsilon^* = \varepsilon' + i\varepsilon''$, was measured using broadband dielectric spectroscopy (BDS). The capacitor was a parallel-plate capacitor with a diameter of 20 mm and a spacer with thickness between 50 and 500 μm . The BDS measurements were performed in the same cryostat [74] and the same setup [75] as the shear mechanical measurements with the PSG, and consequently the temperature control was the same. This enables a direct comparison of the temperatures between the two resulting response functions [70, 76, 77].

Due to the cold-crystallization tendency of some ionic liquids, the protocol for the BDS measurements was to rapidly cool to around T_g and then measure upon heating up until the crystallization sets in. In the liquids with no cold-crystallization, the protocol was to measure while cooling from room temperature and down to around T_g .

The derivative analysis was also implemented in this study. With this analysis, the ohmic conductivity of the ionic liquids is removed from the signal by the use of the relation [78–80]

$$\varepsilon''_{der}(\omega) = -\frac{\pi}{2} \frac{\partial \varepsilon'(\omega)}{\partial \ln(\omega)} \quad (1)$$

This representation of the dielectric permittivity will reveal the main relaxation of the liquid previously hidden underneath the dominating ohmic conductivity signal.

D. Dynamic light scattering

The intensity autocorrelation function $g_2(t)$ was measured in both a vertical-vertical (VV) a vertical-horizontal (VH) geometry in a cold finger cryostat using a fiber optic and a Cobolt Samba 500 Nd:YAG laser at TU Darmstadt. The details of setup and analyses are described in [81]. The $g_2(t)$ function is transformed into the electric field autocorrelation function $g_1(t)$ and then transformed into a generalized susceptibility $\chi(\omega)$ for comparison with other spectroscopy methods [82].

$$\chi''(\omega) = \frac{\omega}{k_b T} \int_{-\infty}^0 g_1(t) e^{-i\omega t} dt \quad (2)$$

The VH geometry setup is also known as Depolarized Dynamic Light Scattering (DDLS) and essentially measures the reorientation of the optical anisotropy tensor of anisotropic molecules. In VV geometry not only molecular reorientation plays a role but also the intermediate scattering function, which reflects density fluctuations on the lengthscale of the optical wavelength used in the experiment [83].

III. RESULTS AND ANALYSIS

A. Shear modulus

Shear mechanical measurements have been performed before on Pyr14-TFSI, Pyr16-TFSI and Pyr18-TFSI [24, 84] as well as Omim-BF4 [32], but not on Pyr18-TFSI mixed with Li-salt and Pmim-BF4. PSG measurements for all seven RTILs have been included in this work for completeness and because the broad frequency range of the PSG method avoids the use of masterplots, although in a limited modulus resolution range. This paper will in the following solely focus on the low frequency part of the shear modulus spectrum.

Figure 3a and 3b show isothermal spectra for the real and imaginary part of the complex shear modulus, respectively, for the six pyrrolidinium-based ionic liquids as well as Omim-BF₄. Data have been scaled in both modulus and frequency to a point in modulus 30% below the toppoint of the alpha relaxation peak, denoted G''_{lf} and ν_{lf} , respectively. For Pyr14-TFSI and Pyr18-TFSI, the shear modulus curve is a combination of results from the PSG and the conventional rheometer measured at the same temperature, where the latter has been scaled slightly in frequency to account for a small temperature off set.

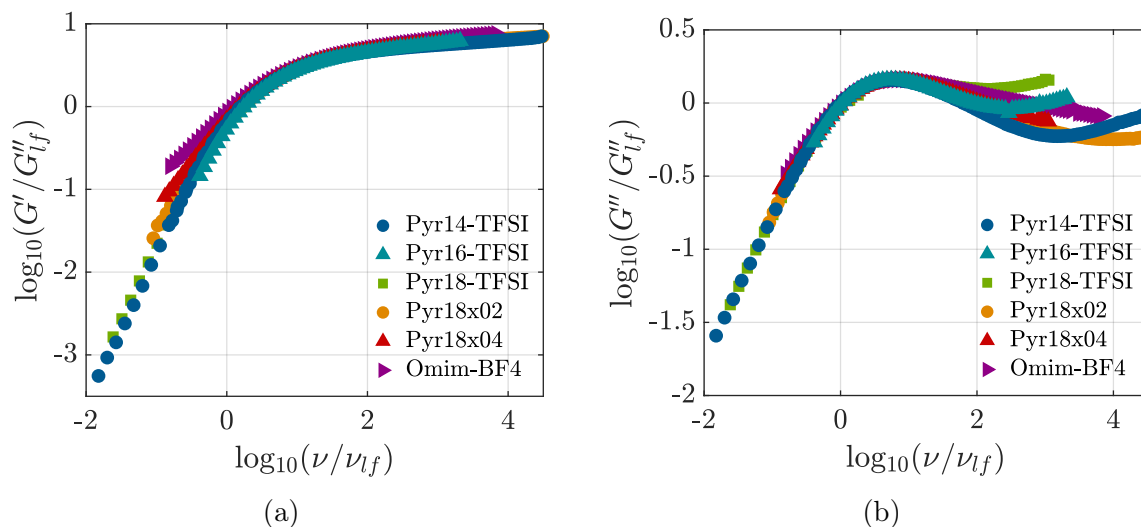


Figure 3: The real (a) and imaginary (b) part of the shear modulus for Pyr1*n*-TFSI with $n = 4, 6$ and 8, Pyr18-TFSI mixed with Li-TFSI in concentrations of 0.2 and 0.4 molar fractions, and Omim-BF₄. Both shear modulus and frequency for all liquids have been scaled to a point in modulus 30% below the toppoint of the alpha relaxation peak (denoted G''_{lf} and ν_{lf}). Data have been measured at 190 K (Pyr14-TFSI), 198 K (Pyr16-TFSI), 200 K (Pyr18-TFSI), 206 K (Pyr18x02), 208 K (Pyr18x04), 202 K (Omim-BF₄) and 180 K (Pmim-BF₄).

Figure 4a and 4b is a zoom in on the real part of the shear modulus, i.e. figure 3a, in order to highlight the low frequency response. Presenting the data this way is an advantage when the presence of a bimodal spectrum is only subtle, since the real part of the shear modulus is especially sensitive to the presence of additional processes. A similar approach was used in the study of low-intensity slow modes in hydrogen-bonding liquids [38]. Furthermore, the data have been divided into two different plots; one with the homologous series of Pyr1*n*-TFSI (a) and the other with Pyr18-TFSI mixed with Li-salt (b). Both plots contain data from Omim-BF₄ and DC704 for comparison. The reason for this comparison is that the Omim-BF₄ contains two modes at lower frequencies [32] and DC704 does not [71]. The black, dashed-dotted line highlights the theoretical expectation for a terminal mode with $G' \propto \nu^2$.

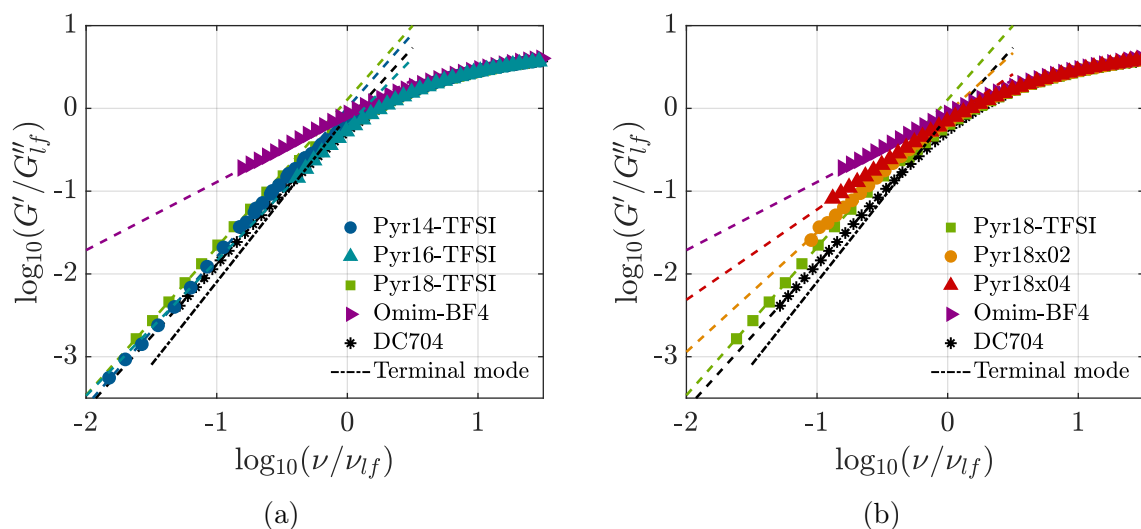


Figure 4: Same data as in figure 3a, i.e. the logarithm of the real (a) part of the shear modulus, but now divided into two plots; a) is Pyr1*n*-TFSI with $n = 4, 6$ and 8 , and b) is Pyr18-TFSI mixed with Li-TFSI in concentrations of 0.2 and 0.4 molar fractions. The shear modulus for Omim-BF4 and DC704 (the latter at 224 K) have been included in both plots for comparison. Dashed lines are linear fits to the low frequency flank of the alpha relaxation peak, and dashed-dotted line is the theoretical expectation for a terminal Maxwell mode with a slope equal to 2 . There is no slow mode in the neat pyrrolidinium-based ionic liquids, but a slow mode appear in both Omim-BF4 and Pyr18-TFSI mixed with Li-salt.

Qualitatively, figure 4a clearly shows the absence of significant slow contributions in Pyr14-TFSI, Pyr16-TFSI and Pyr18-TFSI, since G' reaches the terminal regime right after the alpha relaxation process. This confirms previous investigations of slower modes in Pyr18-TFSI [24]. In Pyr18x02 and Pyr18x04, however, there is a clear deviation from the terminal mode or fully viscous behavior, as seen in figure 4b. This indicates the presence of an additional slower mode in these two liquids, since such a process would give a crossover region from the alpha relaxation to the slow mode (followed by the terminal mode) [41, 85, 86]. It is this crossover which is seen in the low frequency end of the shear modulus spectra for Pyr18x02 and Pyr18x04, but due to the limited range of the PSG measurements at low moduli, the terminal mode is out of reach.

To quantify these results, the slope of the low frequency flank of G' was determined in all of the measured liquids, including DC704. This way of identifying slow modes was also utilized in literature [31, 38]. The method in this work was as follows; identify the frequency range in which the change in $\log_{10}(G')$ as a function of $\log(\nu)$ was constant, by differentiating $\log_{10}(G')$ with respect to $\log_{10}(\nu)$. Then fit the logarithm of G' in this frequency range to a first degree polynomial to obtain the slope.

The resulting slopes for the low frequency flank of G' are presented for all eight liquids in table II. Also shown is the percentage of the slope relative to that of DC704, where there is no slow mode. The reasoning behind this comparison is that, due to experimental uncertainties, the slope of the terminal mode in real liquids does not always reach the theoretical value of 2. A comparison directly with the slope of DC704 will then give a better idea, of whether the terminal mode has been reached for a certain ionic liquid or not.

Liquid	slope G'	% of DC704
DC704	1.75 ± 0.01	100
Pyr14-TFSI	1.80 ± 0.07	103
Pyr16-TFSI	1.6 ± 0.1	91
Pyr18-TFSI	1.79 ± 0.03	103
Pyr18x02	1.45 ± 0.05	83
Pyr18x04	0.99 ± 0.02	57
Pmim-BF ₄	1.22 ± 0.06	70
Omim-BF ₄	0.76 ± 0.01	43

Table II: The slope of the low frequency flank of the real part of the shear modulus for both pyrrolidinium series plus Omim-BF₄, Pmim-BF₄ and DC704.

The resulting slopes in table II show what can also be visually confirmed in figure 4; that there is no slow mode present in either Pyr14-TFSI, Pyr16-TFSI or Pyr18-TFSI. This becomes especially clear when comparing to the result on Omim-BF₄, where the slope is only 0.76, clearly showing the presence of a slow mode. In the series of Pyr18-TFSI mixed with Li-salt, however, a slow mode appears in Pyr18x02, seen as a clear decrease in the slope of G' , and this slow mode increases in intensity in Pyr18x04. Consequently, the addition of Li-salt to Pyr18-TFSI will introduce changes in the dynamics resulting in an additional low-frequency relaxation mode, which increases in intensity with increasing Li-salt concentration.

To further confirm the presence or absence of a bimodal spectrum at lower frequencies, the shear mechanical data are also presented as the imaginary part of the shear viscosity, η'' , where $\eta(\omega)^* = \eta' + i\eta'' = G^*/i\omega$. See figure 5. This representation of shear mechanical data has proven to effectively reveal multimodal behavior in viscous liquids [87], and the two figures clearly confirm the findings from figure 4; that there is only one relaxation

mode at lower frequencies in neat Pyr14-TFSI, Pyr16-TFSI and Pyr18-TFSI, and that an additional relaxation mode appears at lower frequencies when adding Li-salt to Pyr18-TFSI.

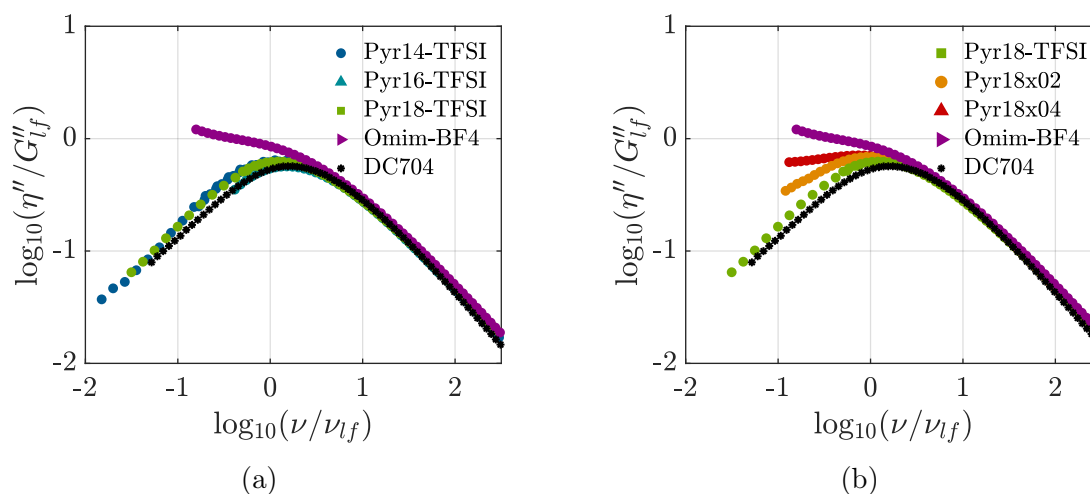


Figure 5: a) and b) show the same shear mechanical data as in figure 4, only this time as the imaginary part of the viscosity, η'' , where $\eta^*(\omega) = \eta'(\omega) + \eta''(\omega)$. The two figures clearly underline the message from figure 4; that there is no slower mode in the neat pyrrolidinium-based ionic liquids, but that there is indeed an additional mode at lower frequencies in Omim-BF4, Pyr18x02 and Pyr18x04, and that the intensity of this additional mode increases with increasing Li-salt concentration.

To expand on this analysis of the slower mode, the shear modulus was in addition measured on Pmim-BF4 and directly compared to results on Omim-BF4, with the latter being from both this study and literature [32], see figure 6a. Here the logarithm of the real part of the shear modulus has again been scaled to the point in modulus 30% below the alpha relaxation peak. The masterplot from literature data was subsequently scaled in both modulus and frequency to match the alpha relaxation peak of the scaled isothermal spectra measured with the PSG. Again, the results on the RTILs were plotted together with results on DC704 for comparison.

The figure shows first of all that the slower mode seen in literature data is also present when measuring with the PSG, seen as a match between the data sets, even though the slope in the shear modulus measured in this work is slightly higher. This match between results from this work and literature also verifies the use of the low frequency slope in identifying a slow mode in the spectrum, when the terminal mode is not within the experimental window.

Second of all, the figure shows that there is also a slower mode present in Pmim-BF4, which is also confirmed by a low-frequency slope in $\log_{10}(G')$ of 1.22, as well as a clear

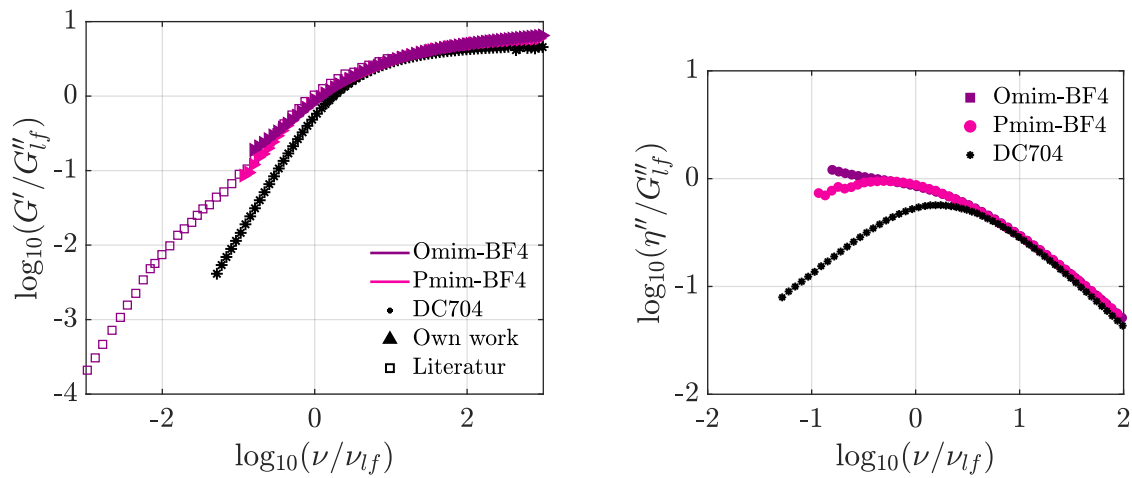


Figure 6: The real part of the shear modulus for Omim-BF4 at 190 K and Pmim-BF4 at 180 K as measured with the PSG together with literature data on Omim-BF4 as measured with a conventional rheometer and shown as a master plot, from [32]. Black asterisks are PSG data from DC704, a simple molecular liquid with no bimodal behavior. It shows the presence of a bimodal spectrum in both Omim-BF4 and Pmim-BF4.

bimodal spectrum in the imaginary part of the viscosity, see figure 6. The absence of a pre-peak in the x-ray structure factor of Pmim-BF4 [54] confirms that a bimodal shear mechanical spectrum in ionic liquids is not necessarily due to a combination of a single alpha relaxation and the relaxation of mesoscale aggregates, since there appears to be no aggregates present in Pmim-BF4.

B. Light Scattering

To gain further insight into the slow mode seen in Pyr18-TFSI with 0.4 molar fraction of Li-TFSI (Pyr18x04), the liquid was measured with DLS. In the DDLS case of light scattering, the measurement of the reorientation of the optical anisotropy tensor relates directly to the reorientation of the main axes of the elongated anion and cation. These are asymmetric in contrast to the very symmetric Li-ion [26], which means that only the asymmetric molecules will give a signal in the results. Consequently, there will be no direct contribution from the Li-ions.

This was quantitatively confirmed by fitting the low-frequency flank of the alpha relaxation to a first degree polynomial for the curves measured at 240 and 235 K. The resulting slopes were 0.99 ± 0.02 and 0.96 ± 0.03 , showing definitely that the terminal mode is reached with no additional sub-alpha relaxations. Furthermore, the alpha relaxation follows a generic shape [71, 88, 89] with a power law behavior of 0.5 at the high-frequency

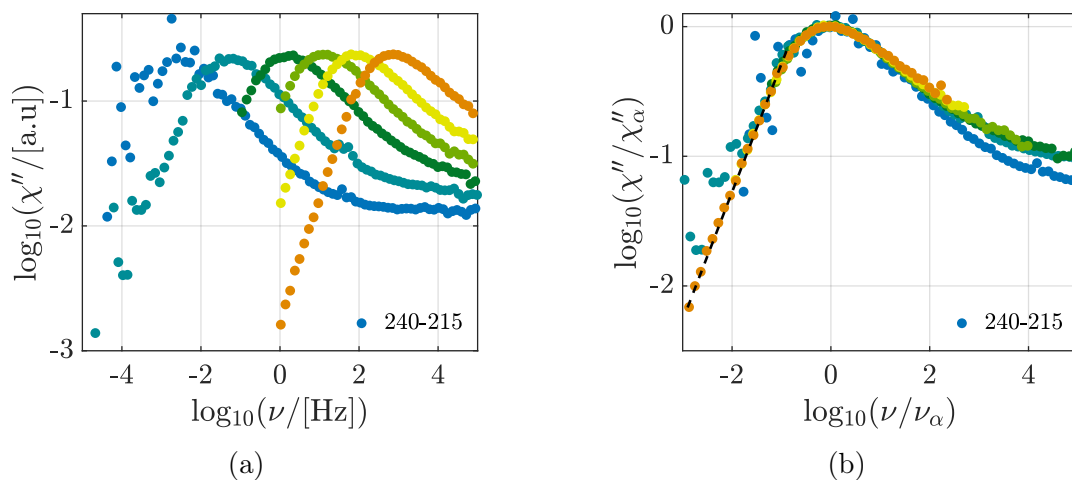


Figure 7: a) The logarithm of DDLs susceptibility of Pyr18x04 measured with the VH setup from 240-215 K in steps of 5 K showing a pronounced alpha relaxation and an excess wing at higher frequencies. b) Same as in a), but with the spectra scaled to the alpha relaxation peak in order to compare the spectral shapes of the curve, showing almost complete TTS except for the high frequency part of the spectrum measured at 215 K. Dashed, black line is a linear fit of the low frequency flank of the alpha relaxation at 240 K. The resulting slope is 0.99, showing that the liquid reaches the terminal mode at all temperatures just after the alpha relaxation.

flank of the peak, strongly indicating no presence of additional processes.

A way to observe the presence of mesoscale aggregates in any liquid measured with light scattering, is to check the difference in the VV and VH correlation functions. In VV geometry, in addition to molecular reorientation, concentration fluctuations of mesoscale aggregates show up as a contribution in the intermediate scattering function [83], in case there is sufficient contrast between the mesoscale objects and their surroundings. However, in the present data of Pyr18x04 VV and VH were found to be identical within uncertainty limits. This means that aggregates are either absent or have too little contrast in refractive index to appear in the intermediate scattering function and thus both measurements identically reflect reorientation.

IV. DISCUSSION

The first point is to assess if the presence or absence of several dynamic modes at lower frequencies in the investigated ionic liquids can be related to the structure factor peak at low Q -values, which is linked to mesoscale aggregates formed by polar and apolar parts of the cation and anion. Starting with the series of pyrrolidinium-based ionic liquids with increasing alkyl chain length, the increase in the pre-peak intensity with increasing alkyl

chain length is not reflected in the slower dynamic mode observed in the shear mechanical spectra. In fact, there is no slow mode in the shear response of any of these three ionic liquids, which challenges view of a ubiquitous slow mode as the dynamic signal of long-lived mesoscale aggregates. This should also be viewed in relation to NMR measurements showing that the concentration of mesoscale aggregates in Pyr1*n*-TFSI increases with increasing alkyl chain length [58]. We also mention, that dielectric measurements at high temperatures in Pyr18-TFSI show bimodal relaxation spectra, which, however, are unrelated to the dynamics of mesoscale aggregates as shown by comparing the pressure dependence of dielectric and SAXS data. On lowering the temperature the slower mode loses intensity so that the dielectric loss becomes monomodal close to T_g [35].

The observed monomodal shear relaxation spectrum in Pyr18-TFSI of this work is in accordance with the above mentioned results in Ref. [35]. However, the finding is surprising in two ways; first that studies on the very similar RTIL Omim-TFSI showed a bimodal spectrum, which was assigned to originate in a time-scale separation of the cation and anion relaxation. This separation appears gradually when increasing the alkyl-chain length of the cation, due to an increased size difference between the two molecules [26]. In Pyr18-TFSI, the size of the cation and anion is comparable to Omim-TFSI, since the anion is identical in the two ionic liquids, and the imidazolium ring with octyl side group is comparable in size to the pyrrolidinium ring with an octyl side group. However, there is no separation of time scales of the cation and anion in Pyr18-TFSI seen in the shear mechanical spectrum, which is puzzling. An explanation could be that the shear response of Pyr18-TFSI is simply too broad to disentangle the time scales separation. In the DDLs response of Omim-TFSI, the separation between the cation and anion relaxation rates was a factor of only around 4.

The second surprising fact is, that there is indeed mesoscale aggregates in this ionic liquid, which one would expect to give a dynamic signal. A low-frequency relaxation mode, which was shown to originate in the mesoscale aggregates, was observed by dynamic light scattering in Omim-BF₄ around 2 decades lower in frequency than the cation alpha relaxation. Pyr18-TFSI was in this work measured 2 decades down in frequency below the alpha relaxation, but with no hint of an even slower relaxation mode. Of course, the slow mode connected to the aggregates could be slower in Pyr18-TFSI than Omim-BF₄, but in any case this underlines once more that the connection between structure and dynamics in RTILs is not a simple matter.

A different picture is drawn with the series of Pyr18-TFSI mixed with Li-TFSI. Here the increase of the pre-peak intensity with increasing Li-salt concentration is reflected in an additional slow relaxation mode which increase in intensity with increasing Li-salt concentration. Furthermore, the pre-peak in Pyr18x02 and Pyr18x04 is of higher intensity than in neat Pyr18-TFSI. This, combined with the absence of a slower mode in the Pyr1*n*-TFSI series, could indicate that the pre-peak intensity needs to be above a certain threshold value, for at slow mode connected to the mesoscale aggregates to be detectable in the shear modulus. This interpretation, of course, assumes that an increase in pre-peak intensity can be directly explained by an increase in the concentration of mesoscale aggregates, since this increase would also affect the signal strength in shear mechanical measurements. However, the increase in the pre-peak intensity with increasing Li-salt concentration could simply be due to an increase in contrast between the polar and apolar regions of the mesoscale aggregates, due to the presence of Li-ions in the polar regions.

Another interpretation is that the appearance of a bimodal spectrum in Pyr18-TFSI mixed with Li-salt is simply due to a separation of time scales. To explain this further, it is important to look at the structure itself. The exchange of pyrrolidinium cations with lithium will introduce significant changes to the microscopic and mesoscopic structure of the ionic liquid. On a microscopic level, NMR and Raman spectroscopy studies on Pyr1*n*-TFSI mixed with Li-TFSI indicates that the TFSI anions coordinates with the Li cations [58]. This significantly affects the dynamics of the anion. Furthermore, it has been shown that one Li-ion and two TFSI anions will form rather stable Li[TFSI]₂ triplets, when the Li-concentration is above ~ 0.1 molar fraction, essentially creating one large, negatively charged cluster [53, 90–92].

To gain more information about the origin of the relaxation dynamics seen in Pyr18x04, the results measured with three different experimental methods, i.e. DMS, BDS and DDLS, are collected into a single plot for a single temperature, see figure 8. More specifically, the figure makes it possible to directly compare the relaxation dynamics from G'' , η'' , χ'' , and ε''_{der} at 230 K. This way of presenting results has been utilized before with success [26].

The figure shows several interesting results, which need to be considered in the interpretation of the multimodal spectrum. The first thing to notice is that the DDLS alpha relaxation peak is slower than the dielectric main relaxation. This is inconsistent with

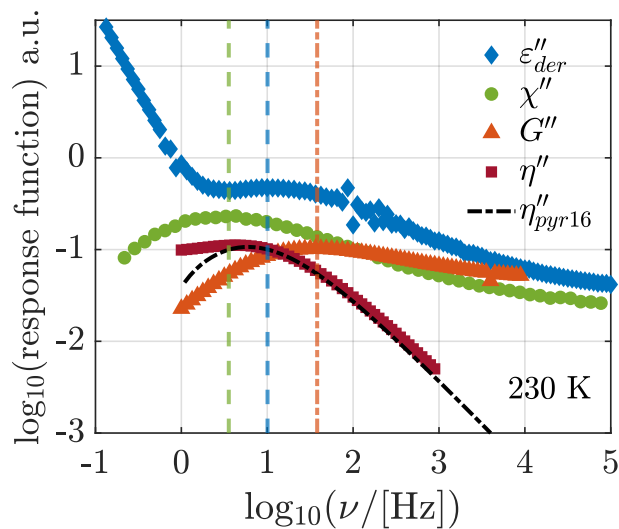


Figure 8: The imaginary part of shear modulus, G'' , shear viscosity, η'' , DDLS susceptibility, χ'' , and the derivative of dielectric permittivity, ϵ''_{der} , measured on Pyr18-TFSI with $x = 0.4$ molar fraction of Li-salt (Pyr18x04). The different response functions show that there is a bimodal spectrum in the shear mechanical spectra, but not in the DDLS and dielectric spectra. For comparison, the imaginary part of the viscosity for Pyr16-TFSI (shifted to collapse with Pyr18x04 viscosity) is shown, since there is only one process in this ionic liquid. Green dashed line is the toppoint of the DDLS peak, blue dashed-line is the toppoint of the derivative of the dielectric permittivity, orange dashed-dotted line is the toppoint of the shear modulus peak.

what is generally observed when comparing the two response functions [82], where the DDLS response is faster than or equal to the dielectric one, due to the difference in Legendre polynomial. Thus, it is a clear indication that the two relaxation modes originate in two separate processes.

These two separate processes could be due to a separation of the rotational and the translational dynamics of the molecules, where the DDLS specifically measures the former, and BDS in principle measures both. However, in the case of Pyr18x04, only the translational, conductivity relaxation process is visible in the dielectric spectrum, as has also been observed in the literature [93].

Following this analysis, it is interesting that there is no multimodal behavior in the dynamic light scattering results, since for the very similar ionic liquids Omim-TFSI and Omim-BF₄, this was clearly the case [26]. Here the two modes arise from a separation of cation-anion relaxation and from a combination of cation and mesoscale aggregate relaxation, respectively. Neither of which is detected in the light scattering results in Pyr18x04 of this work. At first glance, a reason could be the introduction of Li-TFSI which significantly reduces the amount of pyrrolidinium cations, making a possible separation of timescales harder to detect. However, in DDLS even small amounts of anisotropic

molecules that decouple would show as deviations from a generic line shape, which is not observed. Thus, it is clear that the ionic reorientation is one single process, and neither separations in time scales nor bimodal spectra can be explained by different rotational time scales. Therefore, it is most likely that a separation of rotational and translational dynamics is the source of the observed difference in the light scattering and the dielectric response of Pyr18x04. This implies that the bimodal spectrum seen in the shear response likewise originates from a separation of rotation and translational dynamics. It is well known that conductivity decreases and the glass transition moves to lower temperatures when introducing Li TFSI to the Pyr1n-TFSI liquids [91]. In other words all the dynamics slows down. This slowing down is probably related to above mentioned formation of Li[TFSI]₂ triplets [53, 90–92]. In this view introducing Li TFSI would have a slightly different effect on slowing down rotational and translational degrees of freedom leading to the observed separation. Possibly, such a separation of timescales is already present in the neat Pyr1n-TFSI liquids, while not being resolved in the shear mechanical spectrum. A way to investigate further would be to perform measurements with dynamic light scattering on Pyr1n-TFSI as well as Pyr18x02, but this is not possible due to a high degree of cold-crystallization.

The shear mechanical results on Pmim-BF₄ and Omim-BF₄ is another clear indication that the multimodal shear mechanical spectrum is often unrelated to the mesoscale aggregation. Simulation studies of the imidazolium-based RTILs show that an alkyl chain length of less than 4 carbon atoms only show weak mesoscale aggregation [55], and no pre-peak in the structure factor [94]. It was later confirmed that when the alkyl chain is butyl or longer, the alkyl chains will start to interconnect in a bicontinuous, sponge-like structure, forming ordered domains of the polar and apolar parts of the molecules.

Figure 6, however, clearly shows the presence of a bimodal spectrum at lower frequencies in Pmim-BF₄, even though it is less pronounced than in Omim-BF₄. In both cases, decoupling is interpreted to be due to the anion BF₄ being significantly smaller than the cation. This not only leads to a separation of the rotational timescales, but also to a decoupling between rotation and translation, as was demonstrated for Omim-BF₄ in Ref. [16], where the charge relaxation peak in dielectrics is significantly faster than the cation reorientation monitored by DDLS and shear relaxation is bimodal. Moreover, in Fig. 6 it is seen that the slower mode increases in intensity when going from Pmim to Omim. This is in line with the separation between cation-anion time scale increasing with increasing

alkyl chain length.

V. SUMMARY AND CONCLUDING REMARKS

This study has presented shear mechanical results on seven room temperature ionic liquids (RTILs), divided into three different series; 1) a homologous series of Pyr1*n*-TFSI with $n = 4, 6$ and 8 , 2) Pyr18-TFSI mixed with Li-TFSI in molar fractions of 0.2 (Pyr18x02) and 0.4 (Pyr18x04), and 3) C_n -mim-BF₄ with $n = 3$ (Pmim-BF₄) and 8 (Omim-BF₄). The aim was to investigate in detail the origin of the multimodal low-frequency spectra sometimes observed at in RTILs.

Surprisingly, there is no multimodal/bimodal spectrum present in the shear modulus of Pyr18-TFSI, meaning that no dynamic signal from mesoscale aggregates are observed. Furthermore, this result is curious since a bimodal spectrum was observed in literature in Omim-TFSI [26], an ionic liquid with a cation and anion of similar size and composition to the ones in Pyr18-TFSI. The origin of the bimodal spectrum was in that case found to be a time-scale separation of the cation and anion. The absence of this separation in Pyr18-TFSI indicates that replacing the imidazolium ring in Omim with a pyrrolidinium ring in Pyr18 fundamentally changes the dynamics.

A bimodal spectrum was, however, observed in the shear modulus of Pyr18x02 and Pyr18x04, where the slower of the two modes increased in intensity with increasing Li-salt concentration. The same was observed in Pmim-BF₄ and Omim-BF₄, but where the slower mode increased in intensity with increasing alkyl chain length. A comparison of these results with the x-ray structure factor showed that the presence of a pre-peak is not directly linked to the presence of a bimodal spectrum, and so the direct connection between pre-peak intensity and the intensity of the slower mode, which would then have its origin in the mesoscale aggregates, is unlikely in these cases.

Pyr18x04 was studied in further details with the use of dynamic light scattering and dielectric spectroscopy, showing no presence of a bimodal spectrum in these two response function. The one relaxation mode observed in the light scattering spectrum followed a generic alpha relaxation behavior showing that the reorientation of pyrrolidinium cations and TFSI anions is strongly coupled and no signs of aggregate relaxation were found neither in VH nor in VV scattering geometry.

Compared to the dielectric spectrum, the fact that the light scattering relaxation mode is slower than the dielectric strongly indicates that the two observed modes originate in

different molecular processes, most likely a separation of rotational and translational motion, since dynamic light scattering can only observe the first. This separation is also most likely the origin of the bimodal spectrum seen in Pyr18x02 and Pyr18x04.

These specific cases were also further analyzed in a broader perspective, in order to give a more fundamental understanding and overview of the origin of the multimodal spectra observed in ionic liquids. This analysis clearly showed that one needs to take extra care before making the simple and general conclusion, that the slower mode seen in the shear modulus is the dynamic signal of long-lived mesoscale aggregates.

Currently, two explanations for the origin of the bimodal shear mechanical spectra in RTILs are dominating in literature; 1) cation-anion time scale separation or 2) the combined cation-anion relaxation plus the relaxation of mesoscale aggregates. In the present study the most likely picture points towards the first interpretation, combined with the fact, that a separation of timescales also includes a separation of reorientational motion and translational charge relaxation, as in the case of Pyr18x02 and Pyr18x04. But this is clearly elucidated only when comparing the spectra measured across different experimental techniques, e.g. dynamic light scattering and dielectric spectroscopy.

All of this underlines the difficulties of studying RTILs. They are structurally very complex systems with different length- and time-scales, and so far nothing points towards a general, universal origin of the multimodal spectra seen in some ionic liquids when measuring with different experimental techniques. Instead, to understand the underlying mechanisms of a single family of ionic liquids, one needs to use as many strategies as possible, i.e. a large series of ionic liquids with small changes to the chemical structures as well as several, complimentary experimental techniques and computer simulations.

VI. ACKNOWLEDGMENT

This work is part of the project RiDILiq, which is funded by the Independent Research Fund Denmark.

BIBLIOGRAPHY

- [1] B. Scrosati, M. Armand, F. Endres, D. R. MacFarlane, and H. Ohno, "Ionic-liquid materials for the electrochemical challenges of the future," *Nat. Mater.*, vol. 8, no. 8, pp. 621–629, 2009.

- [2] D. R. MacFarlane, M. Kar, and J. M. Pringle, *Fundamentals of ionic liquids: from chemistry to applications*. Newark: Wiley-VCH, 1st ed. ed., 2017.
- [3] B. Kirchner, *Ionic Liquids*. Topics in Current Chemistry, 290, Berlin, Heidelberg: Springer Berlin Heidelberg, 1st ed. 2010. ed., 2010.
- [4] D. R. MacFarlane, *Fundamentals of ionic liquids : from chemistry to applications*. Weinheim, Germany: Wiley-VCH, 2017 - 2017.
- [5] T. Tsuda and C. L. Hussey, “Electrochemical applications of room-temperature ionic liquids,” *The Electrochemical Society Interface*, vol. 16, p. 42, 2007.
- [6] A. Matic and B. Scrosati, “Ionic liquids for energy applications,” *MRS bulletin*, vol. 38, no. 7, pp. 533–537, 2013.
- [7] M. Smiglak, J. M. Pringle, X. Lu, L. Han, S. Zhang, H. Gao, D. R. MacFarlane, and R. D. Rogers, “Ionic liquids for energy, materials, and medicine,” *Chemical communications (Cambridge, England)*, vol. 5, no. 66, pp. 9228–925, 2014.
- [8] A. Wang, W. Yuan, J. Fan, and L. Li, “A dual[Li+TFSI] graphite battery with pure 1-butyl-1-methylpyrrolidinium bis(trifluoromethylsulfonyl) imide as the electrolyte,” *Energy technology (Weinheim, Germany)*, vol. 6, no. 11, pp. 2172–2178, 2018.
- [9] E. Jonsson, “Ionic liquids as electrolytes for energy storage applications – a modelling perspective,” *Energy Storage Materials*, vol. 25, pp. 827–, 2020.
- [10] N. Sun, M. Rahman, Y. Qin, M. L. Maxim, H. Rodríguez, and R. D. Rogers, “Complete dissolution and partial delignification of wood in the ionic liquid 1-ethyl-3-methylimidazolium acetate,” *Green chemistry : an international journal and green chemistry resource : GC*, vol. 11, no. 5, pp. 646–655, 2009.
- [11] S. S. Y. Tan, D. R. MacFarlane, J. Upfal, L. A. Edye, W. O. S. Doherty, A. F. Patti, J. M. Pringle, and J. L. Scott, “Extraction of lignin from lignocellulose at atmospheric pressure using alkylbenzenesulfonate ionic liquid,” *Green chemistry : an international journal and green chemistry resource : GC*, vol. 11, no. 3, pp. 339–345, 2009.
- [12] G. Kaur, H. Kumar, and M. Singla, “Diverse applications of ionic liquids: A comprehensive review,” *J. Mol. Liq.*, vol. 351, pp. 118556–, 2022.
- [13] V. Overbeck, B. Golub, H. Schroeder, A. Appelhagen, D. Paschek, K. Neymeyr, and R. Ludwig, “Probing relaxation models by means of fast field-cycling relaxometry, nmr spectroscopy and molecular dynamics simulations: Detailed insight into the translational

- and rotational dynamics of a protic ionic liquid,” *J. Mol. Liq.*, vol. 319, p. 114207, 2020.
- [14] V. Overbeck, H. Schröder, A.-M. Bónsa, K. Neymeyr, and R. Ludwig, “Insights into the translational and rotational dynamics of cations and anions in protic ionic liquids by means of nmr fast-field-cycling relaxometry,” *Phys. Chem. Chem. Phys.*, vol. 23, no. 4, pp. 2663–2675, 2021.
- [15] J. B. Beckmann, D. Rauber, F. Philippi, K. Goloviznina, J. A. Ward-Williams, A. J. Sederman, M. D. Mantle, A. Pádua, C. W. Kay, T. Welton, *et al.*, “Molecular dynamics of ionic liquids from fast-field cycling nmr and molecular dynamics simulations,” *J. Phys. Chem. B*, vol. 126, no. 37, pp. 7143–7158, 2022.
- [16] C. J. Jafta, C. Bridges, L. Haupt, C. Do, P. Sippel, M. J. Cochran, S. Krohns, M. Ohl, A. Loidl, E. Mamontov, *et al.*, “Ion dynamics in ionic-liquid-based li-ion electrolytes investigated by neutron scattering and dielectric spectroscopy,” *Chem. Sus. Chem.*, vol. 11, pp. 3512–3523, 2018.
- [17] F. Nemoto, M. Kofu, M. Nagao, K. Ohishi, S. Takata, J. Suzuki, T. Yamada, K. Shibata, T. Ueki, Y. Kitazawa, *et al.*, “Neutron scattering studies on short- and long-range layer structures and related dynamics in imidazolium-based ionic liquids,” *J. Chem. Phys.*, vol. 149, no. 5, p. 054502, 2018.
- [18] H. W. Hansen, F. Lundin, K. Adrjanowicz, B. Frick, A. Matic, and K. Niss, “Density scaling of structure and dynamics of an ionic liquid,” *Phys. Chem. Chem. Phys.*, vol. 22, no. 25, pp. 14169–14176, 2020.
- [19] F. Lundin, H. W. Hansen, K. Adrjanowicz, B. Frick, D. Rauber, R. Hempelmann, O. Shebanova, K. Niss, and A. Matic, “Pressure and temperature dependence of local structure and dynamics in an ionic liquid,” *J. Phys. Chem. B*, vol. 125, no. 10, pp. 2719–2728, 2021.
- [20] O. Y. Fajardo, S. Di Lecce, and F. Bresme, “Molecular dynamics simulation of imidazolium c n mim-bf 4 ionic liquids using a coarse grained force-field,” *Phys. Chem. Chem. Phys.*, vol. 22, no. 3, pp. 1682–1692, 2020.
- [21] A. Szabadi, P. Honegger, F. Schöfbeck, M. Sappl, E. Heid, O. Steinhauser, and C. Schröder, “Collectivity in ionic liquids: a temperature dependent, polarizable molecular dynamics study,” *Phys. Chem. Chem. Phys.*, vol. 24, no. 26, pp. 15776–15790, 2022.
- [22] P. A. Knudsen, D. M. Heyes, K. Niss, D. Dini, and N. P. Bailey, “Invariant dynamics in a united-atom model of an ionic liquid,” *J. Chem. Phys.*, vol. 160, no. 3, 2024.

- [23] K. L. Eliassen, H. W. Hansen, F. Lundin, D. Rauber, R. Hempelmann, T. Christensen, T. Hecksher, A. Matic, B. Frick, and K. Niss, “High-frequency dynamics and test of the shoving model for the glass-forming ionic liquid pyr14-tfsi,” *Phys. Rev. Mat.*, vol. 5, p. 065606, 2021.
- [24] W. Tu, G. Szklarz, K. Adrjanowicz, K. Grzybowska, J. Knapik-Kowalczyk, and M. Paluch, “Effect of cation n-alkyl side-chain length, temperature, and pressure on the glass-transition dynamics and crystallization tendency of the [c n c1pyrr]+[tf2n] ionic liquid family,” *J. Phys. Chem. C*, vol. 123, no. 20, pp. 12623–12637, 2019.
- [25] P. J. Griffin, A. P. Holt, K. Tsunashima, J. R. Sangoro, F. Kremer, and A. P. Sokolov, “Ion transport and structural dynamics in homologous ammonium and phosphonium-based room temperature ionic liquids,” *J. Chem. Phys.*, vol. 142, no. 8, pp. 084501–084501, 2015.
- [26] F. Pabst, J. Gabriel, and T. Blochowicz, “Mesoscale aggregates and dynamic asymmetry in ionic liquids: Evidence from depolarized dynamic light scattering,” *J. Phys. Chem. Lett.*, vol. 10, no. 9, pp. 2130–2134, 2019.
- [27] M. Ediger and P. Harrowell, “Perspective: Supercooled liquids and glasses,” *J. Chem. Phys.*, vol. 137, no. 8, 2012.
- [28] K. Niss and T. Hecksher, “Perspective: Searching for simplicity rather than universality in glass-forming liquids,” *J. Chem. Phys.*, vol. 149, no. 23, 2018.
- [29] M. D. Ediger, M. Gruebele, V. Lubchenko, and P. G. Wolynes, “Glass dynamics deep in the energy landscape,” *J. Phys. Chem. B*, vol. 125, no. 32, pp. 9052–9068, 2021.
- [30] V. N. Novikov and A. P. Sokolov, “Temperature dependence of structural relaxation in glass-forming liquids and polymers,” *Entropy*, vol. 24, no. 8, p. 1101, 2022.
- [31] N. V. Pogodina, M. Nowak, J. Lauger, C. O. Klein, M. Wilhelm, and C. Friedrich, “Molecular dynamics of ionic liquids as probed by rheology,” *J. Rheol.*, vol. 55, p. 241, 2011.
- [32] T. Cosby, Z. Vicars, Y. Wang, and J. Sangoro, “Dynamic-mechanical and dielectric evidence of long-lived mesoscale organization in ionic liquids,” *J. Phys. Chem. Lett.*, vol. 8, no. 15, pp. 3544–3548, 2017. PMID: 28715220.
- [33] T. Cosby, U. Kapoor, J. K. Shah, and J. Sangoro, “Mesoscale organization and dynamics in binary ionic liquid mixtures,” *J. Phys. Chem. Lett.*, vol. 10, no. 20, pp. 6274–6280, 2019.
- [34] T. Cosby, M. J. Schnabel, D. P. Durkin, R. A. Mantz, and P. C. Trulove, “Ion dynamics and transport properties of lewis-acidic imidazolium chloroaluminate ionic liquids,” *J. Electrochem. Soc.*, vol. 168, p. 066515, 2021.

- [35] F. Pabst, Z. Wojnarowska, M. Paluch, and T. Blochowicz, “On the temperature and pressure dependence of dielectric relaxation processes in ionic liquids,” *Phys. Chem. Chem. Phys.*, vol. 23, no. 26, pp. 1426–14275, 2021.
- [36] M. Paluch, *Dielectric Properties of Ionic Liquids*. Advances in Dielectrics, Cham: Springer International Publishing AG, 2016.
- [37] P. G. Wolynes and V. Lubchenko, *Dielectric Spectroscopy of Glassy Dynamics*. United States: Wiley, 2012.
- [38] K. Adrjanowicz, B. Jakobsen, T. Hecksher, K. Kaminski, M. Dulski, M. Paluch, and K. Niss, “Communication: Slow supramolecular mode in amine and thiol derivatives of 2-ethyl-1-hexanol revealed by combined dielectric and shear-mechanical studies,” *J. Chem. Phys.*, vol. 143, no. 18, pp. 181102–181102, 2015.
- [39] T. Hecksher, N. B. Olsen, and J. C. Dyre, “Model for the alpha and beta shear-mechanical properties of supercooled liquids and its comparison to squalane data,” *J. Chem. Phys.*, vol. 146, no. 15, pp. 154504–154504, 2017.
- [40] R. Böhmer, C. Gainaru, and R. Richert, “Structure and dynamics of monohydroxy alcohols—milestones towards their microscopic understanding, 100 years after debye,” *Phys. Rep.*, vol. 545, no. 4, pp. 125–195, 2014.
- [41] C. Gainaru, M. Wikarek, S. Pawlus, M. Paluch, R. Figuli, M. Wilhelm, T. Hecksher, B. Jakobsen, J. Dyre, and R. Böhmer, “Oscillatory shear and high-pressure dielectric study of 5-methyl-3-heptanol,” *Colloid Polym. Sci.*, vol. 292, pp. 1913–1921, 2014.
- [42] M. H. Jensen, C. Gainaru, C. Alba-Simionesco, T. Hecksher, and K. Niss, “Slow rheological mode in glycerol and glycerol-water mixtures,” *Phys. Chem. Chem. Phys.*, vol. 2, no. 3, pp. 1716–1723, 2018.
- [43] Z. Song, C. Rodríguez-Tinoco, A. Mathew, and S. Napolitano, “Fast equilibration mechanisms in disordered materials mediated by slow liquid dynamics,” *Sci. Adv.*, vol. 8, no. 15, p. eabm7154, 2022.
- [44] F. Caporaletti and S. Napolitano, “The slow arrhenius process in small organic molecules,” *Phys. Chem. Chem. Phys.*, vol. 26, no. 2, pp. 745–748, 2024.
- [45] P. A. Knudsen, K. Niss, and N. P. Bailey, “Quantifying dynamical and structural invariance in a simple molten salt model,” *J. Chem. Phys.*, vol. 155, no. 5, pp. 054506–054506, 2021.
- [46] J. C. Araque, J. J. Hettige, and C. J. Margulis, “Modern room temperature ionic liquids, a simple guide to understanding their structure and how it may relate to dynamics,” *J. Phys.*

- Chem. B*, vol. 119, no. 40, pp. 12727–12740, 2015.
- [47] E. W. Castner and J. F. Wishart, “Spotlight on ionic liquids,” *J. Chem. Phys.*, vol. 132, no. 12, pp. 120901–120901–9, 2010.
- [48] H. K. Kashyap, C. S. Santos, N. S. Murthy, J. J. Hettige, K. Kerr, S. Ramati, J. Gwon, M. Gohdo, S. I. Lall-Ramnarine, J. F. Wishart, C. J. Margulis, and E. W. Castner, “Structure of 1-alkyl-1-methylpyrrolidinium bis(trifluoromethylsulfonyl)amide ionic liquids with linear, branched, and cyclic alkyl groups,” *J. Phys. Chem. B*, vol. 117, no. 49, pp. 15328–15337, 2013.
- [49] A. Triolo, O. Russina, H.-J. Bleif, and E. Di Cola, “Nanoscale segregation in room temperature ionic liquids,” *J. Phys. Chem. B*, vol. 111, no. 18, pp. 4641–4644, 2007.
- [50] A. Triolo, O. Russina, B. Fazio, G. B. Appetecchi, M. Carewska, and S. Passerini, “Nanoscale organization in piperidinium-based room temperature ionic liquids,” *J. Chem. Phys.*, vol. 130, no. 16, p. 164521, 2009.
- [51] L. Song, B. J. Leobardo, G. Jianchang, A. Lawrence, R. Gernot, S. R. W, H. P. C, D. Sheng, B. G. A, and C. P. T, “Alkyl chain length and temperature effects on structural properties of pyrrolidinium-based ionic liquids: A combined atomistic simulation and small-angle x-ray scattering study,” *J. Phys. Chem. Lett.*, vol. 3, no. 1, pp. 125–130, 2012.
- [52] K. Shimizu, C. E. S. Bernardes, and J. N. Canongia Lopes, “Structure and aggregation in the 1-alkyl-3-methylimidazolium bis(trifluoromethylsulfonyl)imide ionic liquid homologous series,” *J. Phys. Chem. B*, vol. 118, no. 2, pp. 567–576, 2014.
- [53] L. Aguilera, J. Vlkner, A. Labrador, and A. Matic, “The effect of lithium salt doping on the nanostructure of ionic liquids,” *Phys. Chem. Chem. Phys.*, vol. 17, no. 40, pp. 27082–27087, 2015.
- [54] O. Russina, A. Triolo, L. Gontrani, and R. Caminiti, “Mesoscopic structural heterogeneities in room-temperature ionic liquids,” *J. Phys. Chem. Lett.*, vol. 3, no. 1, pp. 27–33, 2012.
- [55] R. Hayes, G. G. Warr, and R. Atkin, “Structure and nanostructure in ionic liquids,” *Chem. Rev.*, vol. 115, no. 13, pp. 6357–6426, 2015.
- [56] P. J. Griffin, A. P. Holt, Y. Wang, V. N. Novikov, J. R. Sangoro, F. Kremer, and A. P. Sokolov, “Interplay between hydrophobic aggregation and charge transport in the ionic liquid methyltrioctylammonium bis(trifluoromethylsulfonyl)imide,” *J. Phys. Chem. B*, vol. 118, no. 3, pp. 783–790, 2014.

- [57] A. Martinelli, A. Matic, P. Jacobsson, L. Börjesson, A. Fernicola, and B. Scrosati, "Phase behavior and ionic conductivity in lithium bis(trifluoromethanesulfonyl)imide-doped ionic liquids of the pyrrolidinium cation and bis(trifluoromethanesulfonyl)imide anion.," *J. Phys. Chem. B*, vol. 113, no. 32, pp. 11247–11251, 2009.
- [58] M. Kunze, S. Jeong, E. Paillard, M. Schonhoff, M. Winter, and S. Passerini, "New insights to self-aggregation in ionic liquid electrolytes for high-energy electrochemical devices," *Adv. Energy Mater.*, vol. 1, no. 2, pp. 274–281, 2011.
- [59] K. R. Harris, L. A. Woolf, M. Kanakubo, and T. Rütther, "Transport properties of N-butyl-N-methylpyrrolidinium bis(trifluoromethylsulfonyl)amide," *Journal of Chemical & Engineering Data*, vol. 56, no. 12, pp. 4672–4685, 2011.
- [60] F. M. Vitucci, D. Manzo, M. A. Navarra, O. Palumbo, F. Trequattrini, S. Panero, P. Bruni, F. Croce, and A. Paolone, "Low-temperature phase transitions of 1-butyl-1-methylpyrrolidinium bis(trifluoromethanesulfonyl)imide swelling a polyvinylidene fluoride electrospun membrane," *J. Phys. Chem. C*, vol. 118, no. 11, pp. 5749–5755, 2014.
- [61] K. R. Harris and M. Kanakubo, "Self-diffusion, velocity cross-correlation, distinct diffusion and resistance coefficients of the ionic liquid [bmim][tf2n] at high pressure," *Phys. Chem. Chem. Phys.*, vol. 17, pp. 23977–23993, 2015.
- [62] E. Zorebski, M. Zorebski, M. Dzida, P. Goodrich, and J. Jacquemin, "Isobaric and isochoric heat capacities of imidazolium-based and pyrrolidinium-based ionic liquids as a function of temperature: Modeling of isobaric heat capacity," *Industrial & Engineering Chem. Research*, vol. 56, no. 9, pp. 2592–2606, 2017.
- [63] R. Ge, C. Hardacre, J. Jacquemin, P. Nancarrow, and D. W. Rooney, "Heat capacities of ionic liquids as a function of temperature at 0.1 mpa. measurement and prediction," *J. Chem. Eng. Data*, vol. 53, no. 9, pp. 2148–2153, 2008.
- [64] E. W. Castner, J. F. Wishart, and H. Shirota, "Intermolecular dynamics, interactions, and solvation in ionic liquids," *Acc. Chem. Res.*, vol. 40, no. 11, pp. 1217–1227, 2007.
- [65] H. Shirota, A. M. Funston, J. F. Wishart, and E. W. Castner, Jr, "Ultrafast dynamics of pyrrolidinium cation ionic liquids," *J. Chem. Phys.*, vol. 122, no. 18, pp. 184512–184512, 2005.
- [66] A. Stoppa, O. Zech, W. Kunz, and R. Buchner, "The conductivity of imidazolium-based ionic liquids from (-35 to 195) c. a. variation of cations alkyl chain," *J. Chem. Eng. Data*, vol. 55, no. 5, pp. 1768–1773, 2010.

- [67] C. S. Santos, N. S. Murthy, G. A. Baker, and E. W. Castner, “Communication: X-ray scattering from ionic liquids with pyrrolidinium cations,” *J. Chem. Phys.*, vol. 134, no. 12, pp. 121101–121101–4, 2011.
- [68] B. Jakobsen, A. Sanz, K. Niss, T. Hecksher, I. H. Pedersen, T. Rasmussen, T. Christensen, N. B. Olsen, and J. C. Dyre, “Thermalization calorimetry: A simple method for investigating glass transition and crystallization of supercooled liquids,” *AIP advances*, vol. 6, no. 5, pp. 55019–055019–16, 2016.
- [69] B. Jakobsen, K. Niss, and N. B. Olsen, “Dielectric and shear mechanical alpha and beta relaxations in seven glass-forming liquids,” *J. Chem. Phys.*, vol. 123, p. 234511, 2005.
- [70] L. A. Roed, J. C. Dyre, K. Niss, T. Hecksher, and B. Riechers, “Time-scale ordering in hydrogen- and van der waals-bonded liquids,” *J. Chem. Phys.*, vol. 154, no. 18, pp. 184508–184508, 2021.
- [71] T. Hecksher, N. B. Olsen, and J. C. Dyre, “Rheological model for the alpha relaxation of glass-forming liquids and its comparison to data for dc704 and dc705,” *J. Chem. Phys.*, vol. 156, no. 19, pp. 194502–194502, 2022.
- [72] T. Christensen and N. B. Olsen, “A rheometer for the measurement of a high shear modulus covering more than seven decades of frequency below 50 khz,” *Rev. Sci. Instrum.*, vol. 66, no. 10, pp. 5019–5031, 1995.
- [73] M. Mikkelsen, K. L. Eliassen, N. Lindemann, K. Moch, R. Böhmer, H. A. Karimi-Varzaneh, J. Lacayo-Pineda, B. Jakobsen, K. Niss, T. Christensen, and T. Hecksher, “Piezo-electric shear rheometry: Further developments in experimental implementation and data extraction,” *J. Rheol.*, vol. 66, no. 5, 2022.
- [74] B. Igarashi, T. Christensen, E. H. Larsen, N. B. Olsen, I. H. Pedersen, T. Rasmussen, and J. C. Dyre, “A cryostat and temperature control system optimized for measuring relaxations of glass-forming liquids,” *Rev. Sci. Instrum.*, vol. 79, no. 4, p. 045105, 2008.
- [75] B. Igarashi, T. Christensen, E. H. Larsen, N. B. Olsen, I. H. Pedersen, T. Rasmussen, and J. C. Dyre, “An impedance-measurement setup optimized for measuring relaxations of glass-forming liquids,” *Rev. Sci. Instrum.*, vol. 79, no. 4, p. 045106, 2008.
- [76] C. Gainaru, T. Hecksher, N. B. Olsen, R. Böhmer, and J. C. Dyre, “Shear and dielectric responses of propylene carbonate, tripropylene glycol, and a mixture of two secondary amides,” *J. Chem. Phys.*, vol. 137, no. 6, pp. 064508–064508, 2012.

- [77] B. Jakobsen, T. Hecksher, T. E. Christensen, N. B. Olsen, J. C. Dyre, and K. Niss, "Identical temperature dependence of the time scales of several linear-response functions of two glass-forming liquids," *J. Chem. Phys.*, vol. 136, p. 081102, 2012.
- [78] C. J. F. Böttcher and P. Bordewijk, *Theory of Electric Polarization*, vol. II of *Dielectrics in time-dependent fields*. Amsterdam: Elsevier, 2nd, completely revised ed., 1980.
- [79] M. Wübbenhorst and J. van Turnhout, "Analysis of complex dielectric spectra. i. one-dimensional derivative techniques and three-dimensional modelling," *J. Non-Cryst. Solids*, vol. 305, no. 1, pp. 40–49, 2002.
- [80] F. Kremer and A. Schönhal, eds., *Broadband dielectric spectroscopy*. Berlin: Springer, 2003.
- [81] G. Jan, P. Florian, and B. Thomas, "Debye process and beta-relaxation in 1-propanol probed by dielectric spectroscopy and depolarized dynamic light scattering," *J. Physical Chem. B*, vol. 121, no. 37, pp. 8847–8853, 2017.
- [82] J. Gabriel, F. Pabst, A. Helbling, T. Böhmer, and T. Blochowicz, *Depolarized Dynamic Light Scattering and Dielectric Spectroscopy: Two Perspectives on Molecular Reorientation in Supercooled Liquids*, pp. 203–245. Cham: Springer International Publishing, 2018.
- [83] B. J. Berne, *Dynamic light scattering : with applications to chemistry, biology and physics*. Mineola, N.Y: Dover, 2000.
- [84] O. Palumbo, F. Trequattrini, F. M. Vitucci, and A. Paolone, "Relaxation dynamics and phase transitions in ionic liquids: Viscoelastic properties from the liquid to the solid state," *J. Phys. Chem. B*, vol. 119, no. 40, pp. 12905–12911, 2015.
- [85] C. Gainaru, M. Wikarek, S. Pawlus, M. Paluch, R. Figuli, M. Wilhelm, T. Hecksher, B. Jakobsen, J. C. Dyre, and R. Böhmer, "Oscillatory shear and high-pressure dielectric study of 5-methyl-3-heptanol," *Colloid Polym. Sci.*, vol. 292, no. 8, pp. 1913–1921, 2014.
- [86] T. Hecksher and B. Jakobsen, "Communication: Supramolecular structures in monohydroxy alcohols: Insights from shear-mechanical studies of a systematic series of octanol structural isomers," *J. Chem. Phys.*, vol. 141, no. 10, pp. 101104–101104, 2014.
- [87] S. Arrese-Igor, A. Alegría, and J. Colmenero, "Multimodal character of shear viscosity response in hydrogen bonded liquids," *Phys. Chem. Chem. Phys.*, vol. 20, no. 44, pp. 27758–27765, 2018.
- [88] A. I. Nielsen, T. Christensen, B. Jakobsen, K. Niss, N. B. Olsen, R. Richert, and J. C. Dyre, "Prevalence of approximate τ relaxation for the dielectric α process in viscous organic liquids," *J. Chem. Phys.*, vol. 130, p. 154508, 04 2009.

This is the author's peer reviewed, accepted manuscript. However, the online version of record will be different from this version once it has been copyedited and typeset.
PLEASE CITE THIS ARTICLE AS DOI: 10.1063/5.0215661

- [89] P. Florian, G. J. Philipp, B. Till, W. Peter, H. Andreas, R. Timo, Z. Parvaneh, W. Thomas, and B. Thomas, "Generic structural relaxation in supercooled liquids," *J. Phys. Chem. Lett.*, vol. 12, no. 14, pp. 3685–3690, 2021.
- [90] L. Jean-Claude, G. Joseph, A. Christian, and J. Patrik, "Spectroscopic identification of the lithium ion transporting species in litfsi-doped ionic liquids," *J. Phys. Chem. A*, vol. 113, no. 1, pp. 305–314, 2009.
- [91] J. Pitawala, A. Martinelli, P. Johansson, P. Jacobsson, and A. Matic, "Coordination and interactions in a li-salt doped ionic liquid," *J. Non-Cryst. Solids*, vol. 407, pp. 318–323, 2015.
- [92] K. Pilar, V. Balédent, M. Zeghal, P. Judeinstein, S. Jeong, S. Passerini, and S. Greenbaum, "Communication: Investigation of ion aggregation in ionic liquids and their solutions with lithium salt under high pressure," *J. Chem. Phys.*, vol. 148, no. 3, pp. 031102–031102, 2018.
- [93] C. A. Thomann, P. Münzner, K. Moch, J. Jacquemin, P. Goodrich, A. P. Sokolov, R. Böhrmer, and C. Gainaru, "Tuning the dynamics of imidazolium-based ionic liquids via hydrogen bonding. i. the viscous regime," *J. Chem. Phys.*, vol. 153, no. 19, pp. 194501–194501, 2020.
- [94] S. M. Urahata and M. C. Ribeiro, "Structure of ionic liquids of 1-alkyl-3-methylimidazolium cations: A systematic computer simulation study," *J. Chem. Phys.*, vol. 120, no. 4, pp. 1855–1863, 2004.